Int. J. Electrochem. Sci., 14 **(2019)** 6257 – 6266, doi: 10.20964/2019.07.07

International Journal of
ELECTROCHEMICAL
SCIENCE
www.electrochemsci.org

The Effect of Air on Electrochemical Behavior of Activated Carbon at Negative Potentials in Aqueous Li_2SO_4 Electrolyte

J. Ping[1], *S. Rauf*[1], *S.Y. Huang*[1], *W.S. Li*[1], *S.H. Liang*[1], *R.L. Wang*[1], *Q.A. Huang*[2,**], *V.V. Morchenkov*[3], *C.P. Yang*[1,*]

[1] Faculty of Physics and Electronic Technology, Hubei University
[2] College of Science / Institute for Sustainable Energy, Shanghai University, Shanghai 200444, China
[3] Institute of Metal Physics Ural Branch of the Russian Academy of Sciences, 620990, Ekaterinburg, Russia
[*]E-mail: 1042938556@qq.com (C.P. Yang), hqahqahqa@163.com (Q.A. Huang)

Received: 13 January 2019 / *Accepted:* 28 March 2019 / *Published:* 10 June 2019

The electrochemical behavior of activated carbon (AC) has been studied in the presence of air at negative potentials in 0.5M Li_2SO_4 aqueous electrolyte applying the linear sweep voltammetry (LSV). The AC electrodes of low mass loading are disposed and found with distorted LSV curves at constant scan rate, rather than formation of symmetric rectangular shape. Such unusual phenomenon for AC in the electrolyte exposed to air alternatively can be reflected by the discharge capacity of 145 mAh/g with a pretty high coulombic efficiency (332%) obtained in the galvanostatic charge-discharge (GCD) test. Meanwhile, the variation in current with scan rate at fixed potentials corresponds to the remarkable deviation of exponent in the power-law equation from the value 1. The oxidative effect of O_2 and H_2O is investigated to explain the abnormal electrochemical behavior of AC. In the vessel with N_2 flow, AC turns to exhibit recognizable capacitive behavior without considering residual dissolved oxygen in the electrolyte. The self-discharging of AC from 0V to around -0.2V without any external bias is observed in the electrolyte of low level of dissolved oxygen. The above results show the improved electrochemical stability of AC in the absence of air, providing information of value based on application for aqueous lithium-ion hybrid supercapacitors using AC anode.

Keywords: activated carbon (AC); linear sweep voltammetry (LSV); air; oxidative effect; self-discharging; electrochemical stability

1. INTRODUCTION

Hybrid capacitors (HCs) combine the charge storage mechanisms of both electrostatic and electrochemical capacitance and received much attention these years [1]. Lithium-ion hybrid supercapacitors (LIHSs) as an offshoot of HCs have been developed to bridge the gap between electric

double layer capacitors (EDLCs) and lithium-ion batteries (LIBs) [2-5]. The LIHSs in general employed a lithium-ion intercalation electrode with an electric double layer capacitance electrode in an electrolyte containing lithium ions in a single device. Such configuration overcomes the energy density limitations of the EDLCs and the power density limitations of LIBs. Many researchers have turned their directions to develop aqueous lithium-ion hybrid supercapacitors (ALIHSs) which operate in aqueous electrolytes instead of organic ones based on safe and cost effectiveness [6-9]. It is widely accepted that carbon based materials have been commonly used as capacitor-type electrode materials for LIHSs due to large surface area, high conductivity, relatively low cost, high chemical stability, and well-established electrochemistry [1,10]. Therefore, carbon materials are available in different forms such as activated carbon (AC) [11-13], carbon nanotube (CNT) [14-15] and graphene [16] etc. However, activated carbon has been considered representative widely utilized in ALIHSs [17-21].

It is known that an electrode exhibiting electric double layer capacitance stores its charge electrostatically without transfer of charge between the electrolyte and electrode [11]. In this consequence, many limitations of the performance of capacitor-type (non-faradaic) electrode materials have been reported and there exist a concern with the properties of the interface between the electrolytes and electrodes [10, 22-24]. For example, previous study explained that AC exhibited capacitive behavior in aqueous electrolytes containing differing alkali ions and discussed the effect of the hydrated ionic radii on the rate behaviors of AC as well as ionic dynamic dispersion within the pores of AC [23]. It has been believed that there is no adverse influence on the performance of the cathode; AC became a candidate material for anode of the two-electrode system used to test cycling performance of various cathode materials for aqueous rechargeable lithium ion batteries [25-27]. However, in the present work, we investigated the electrochemical behavior of AC at negative potentials in aqueous Li_2SO_4 electrolyte and for the first time we experimentally demonstrated that air can also have an effect on the non-faradaic process occurring on the surface of AC. The results showed that the electrolyte free from air could obviously improve the performance of AC, providing information of value concerned with the practical use of AC in ALIHSs application.

2. EXPERIMENTAL

Activated carbon (YEC-8A from Fuzhou Yihuan carbon Co., Ltd., specific surface area, > 2100 m^2/g, used as received without further treatment) used as a working electrode material. The activated carbon (AC) electrode was prepared by pressing a powder mixture of AC, acetylene black (Taiyuan LZY Battery Sales Department, battery grade) and poly (tetrafluoroethylene) (PTFE) (Shanghai Aladdin Biochemical Technology Co., Ltd., Polytetrafluoroethylene preparation, 60 wt% dispersion) in a weight ratio of 75 : 15 : 10 on stainless steel grid at 10MPa. The electrolyte was of 0.5 M Li_2SO_4. All the electrochemical tests of the individual electrode were performed using a three-electrode system in an electrochemical glass cell with and without N_2 flow where AC was used as counter and saturated calomel electrode (SCE) as reference electrode. It was considered that before every tests, each freshly prepared electrode was conditioned by cycling at 50 mV/s ~ 20 times in a potential window of 0 to -0.85V (vs. SCE), to wet and remove trace amounts of air from the structure of the electrodes. Cathodic linear sweep

voltammetric data were collected by sweeping the potential from 0 to -0.85 V after conditioning the electrode at 0 V for 10min. The aim of the voltage hold step is to balance the entire inner surface electroactivity of the electrode at the initial potential before each scan. The anodic scan was performed from -0.85 to 0V and was collected after keeping the working electrode at -0.85V for 10 min. The galvanostatic charge-discharge test was conducted within a potential window of -0.85 to 0 V. The open circuit potential was recorded after keeping the working electrode at 0V for 10min.

3. RESULTS AND DISCUSSION

The cathodic and anodic LSV curves as a function of mass loading of same size (1.96 cm^2) AC electrodes containing above mentioned ratios of mixture of AC, acetylene black and PTFE for two scan rates displayed in Fig 1. It was observed that the LSV curves for the electrodes of mass loading higher than 10 mg exhibited rectangular shape at the slow scan rate of 0.5mV/s depicted in Fig 1a. Furthermore, the distortion of LSV curves were noticed for the decrease in mass loading especially for 5 and 2.1 mg and furthermore, the negative currents was witnessed from the beginning of the anodic scan. In the meantime, in each case the capacity was irreversible which was calculated based on integrating the LSV curve respectively for cathodic and anodic scans to obtain the voltammetric charge. The scan rate has played a key role in recovering the reversible capacitive behavior, the scan rate was doubled shown in Fig 1b as well presented in Fig 1a. It shows that the increase of scan rate has made distortion phenomenon less obvious in curve. However, scan rate of 1 mV/s was still not strong enough to convert the distorted LSV curves for the mass loading of 2.1 mg to obtain a symmetric rectangular shape in spite of the absence of negative currents in the anodic scan. At this stage, it was found that the distortion of LSV curves could be more easily observed for AC electrode of mass loading less than 2.1mg at a low scan rate (< 1mV/s) and varying the scan rate has an impact on the voltammetric relationship between current and potential.

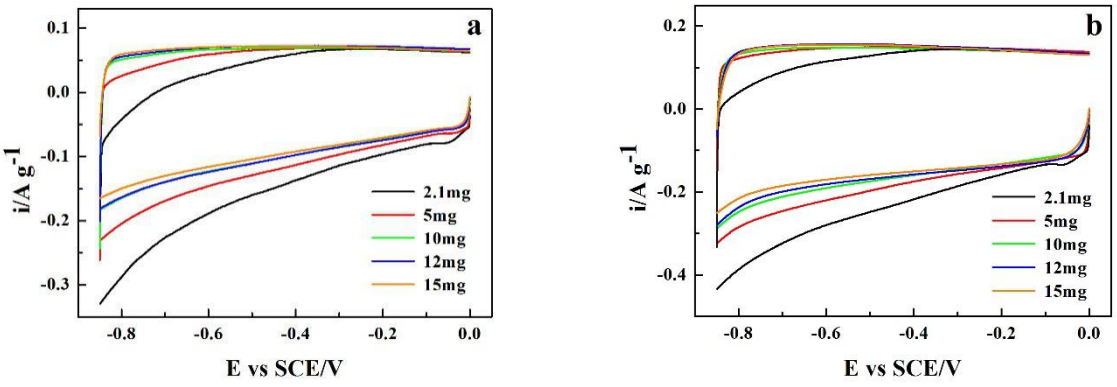

Figure 1. Cathodic and anodic linear sweep voltammetry curves as a function of mass loading of Activated carbon electrodes of the same size for two scan rate (a) 0.5mV/s; (b) 1mV/s in 0.5M Li_2SO_4 solution within a potential window of 0 to -0.85V.

It has been demonstrated that the discharged state of lithium-ion intercalated compounds of all

anode materials suitable for aqueous lithium-ion batteries without exception reacts with water and O_2 [28]. Luo et al. obtained the cyclic voltammograms of $LiTi_2PO_4$ with 1M Li_2SO_4 solution exposed to air where the redox peak current decreased with the increasing of cycle number, thus resulting in the capacity fading upon cycling. They claimed that the chemical oxidation of water and O_2 was responsible for deterioration of the cycling stability of $LiTi_2PO_4$. However, as an anode material restoring charges electrostatically in aqueous Li_2SO_4 solution, AC exhibited the unusual electrochemical behavior described above accompanied by the deteriorated performance. Initially, we proposed that the effect of air was the main cause of the curve distortion because only purely non-faradaic currents were involved in the AC electrode before H_2 evolution as indicated by the fact that no cathodic and anodic peaks were witnessed in the curves displayed in Fig. 1. The following reaction would be expected to occur:

$$(1/4)\ O_2 + (1/2)\ H_2O + e^- ==== OH^-$$

As the potential decreases, the discharged AC will be more easily subject to a state prone to loss of electron. On the other hand, a low mass loading (< 2.1mg) with a relatively low electron reservoir at a fixed potential will also render the reaction more detectable in terms of the specific current density under the condition if content of oxygen dissolved in electrolyte would be constant.

In order to get more in deep knowledge of voltammetric relationship between current and potential, the scan rate was maintained within a range of 0.1 – 1 mV/s and 10 cathodic and anodic scans were carried out in a three-electrode system with and without N_2 flow for the AC electrode of mass loading of 2.1 mg. In the same manner, it has been described above (Fig 1), all the LSV curves obtained in the electrolyte exposed to air at different degrees, suffer the distortion shown in Fig. 2a, which can also be reflected by the fact that the reversible portion of the capacity decreases with the decreasing of scan rate. Nonetheless, the existence of negative currents in anodic scans are common at scan rate below 1 mV/s, and the curve for the scan rate of 0.1mV/s has been completely swallowed by negative currents. Whereas, in the case of N_2 flow into the electrolyte (Fig. 2b), all the curves exhibited nearly symmetric rectangular shape. The current also changed regularly with the increasing of scan rate. The inconsistency of pattern between the two pictures was investigated by analyzing how the current (I) changed with the scan rate (V) at a fixed potential.

The variation of the cathodic current and anodic current at the -0.8 and -0.25 V respectively with scan rate maintained within 0.1 – 1 mV/s for the AC electrode of mass loading of 2.1 mg in the electrochemical glass cell with and without N_2 flow is shown in Fig. 2c. Assuming that the current obeys a power-law relationship with the scan rate leads following the relationship [19, 29, 30]:

$$i = av^b$$

Where a and b are adjustable values. Fitting the point data in the equation gives b values of 1.24 and 0.44 respectively for the anodic and cathodic currents in the presence of air while the calculated b values for the N_2 flow in electrochemical glass cell correspondingly varies from 0.98 to 0.71. The possible reason why a simple power function can fit the data quite well presented in Fig 2c is quite simple that the scan rate was varied within 1 order of magnitude [29]. In more detail, data has been presented in Fig 2d, where the b values at different potentials for both the cathodic and anodic scans have been shown for the AC electrode of mass loading of 2.1mg in the electrochemical glass cell with and without N_2 flow. Herein, we only presented the data including the hollow circle due to the negative

current involved in the anodic scans in Fig 1a that result in a lack of the anodic current data for fitting and unable to give the missing b values. In this consequence, a simple estimation of missing values has been mentioned below appropriately.

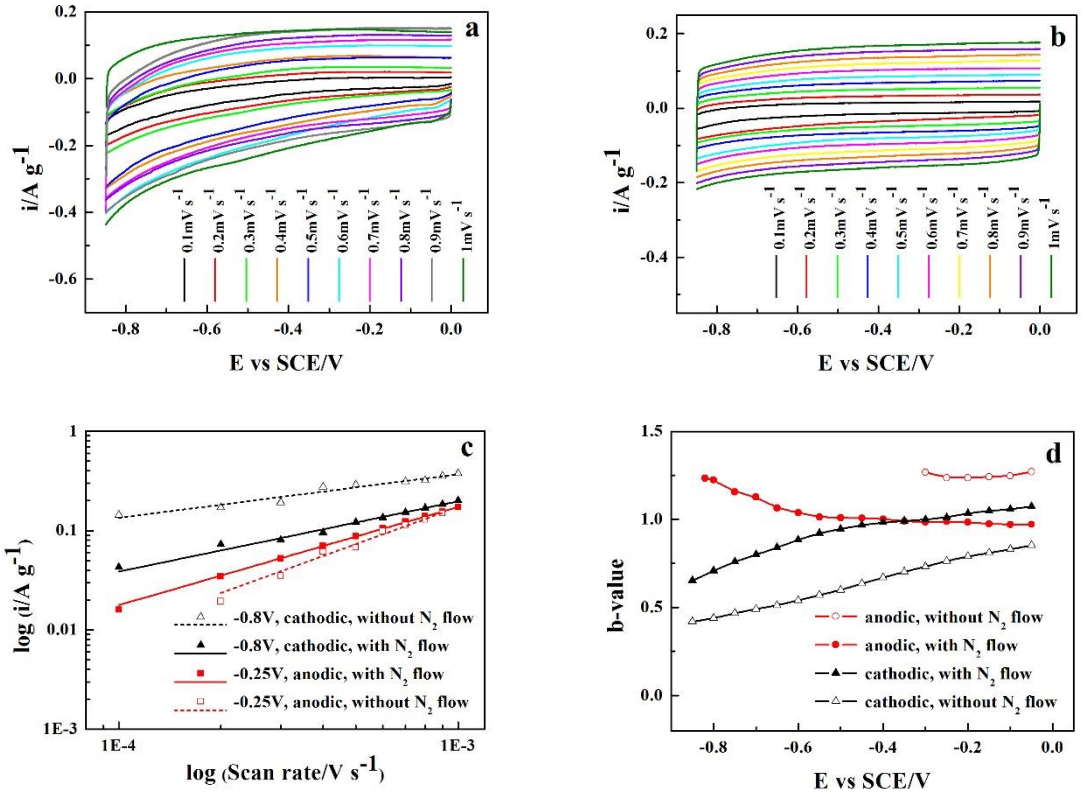

Figure 2. Cathodic and anodic linear sweep voltammetry curves as a function of scan rate for the Activated carbon electrode of mass loading of 2.1mg in 0.5M Li_2SO_4 solution (a) exposed to air; (b) with N_2 flow within a potential window of 0 to -0.85V ; (c) A log-log plot of the obtained currents at -0.8 and -0.25V at different scan rates maintained within a range of 0.1 - 1mV/s, respectively for cathodic and anodic currents in the cases of with and without N_2 flow; (d) calculated b values plotted vs. potential for cathodic and anodic currents in (a) and (b).

To test the electrolyte exposed to air, the b values for cathodic scan were smaller than 1, while the opposite values were obtained in the case for anodic scan. After introducing the N_2 flow, both two profiles of solid point as compared to their counterparts of hollow point (Fig 2d), become closer to the axis, b = 1, and intersect with each other.

The variation of the b values can be explained in terms of faradaic and non-faradaic currents; 'b' value of 0.5 would indicate that the current is controlled by semi-infinite linear diffusion, while value of 1 indicates that the current is surface-controlled [19, 29, 30]. Customarily, the charge storage on AC electrodes occurred through the non-faradaic adsorption at the interfaces between the electrodes and electrolyte. For this reason, the remarkable deviation in the values b from 1 at various potentials observed in the case of absence of N_2 flow. It was supposed to be associated with the chemically oxidative effect of O_2 and H_2O rather than the electrochemical redox process. However, it was evaluated that b values

for both cathodic and anodic scan still tends to deviate from 1 at low potentials in a symmetrical manner depicted by solid point in Fig 2d to the left of the intersection, which could be the result of the insufficient elimination of dissolved oxygen in aqueous Li_2SO_4 electrolyte. Herein, we probably extrapolated the hollow circles at potentials lower than -0.3V from the trend of hollow triangles in Fig 2d, the extrapolated b values would likely form a profile symmetric with that of hollow triangle. As the potential approaches 0V, the shrinking distances from solid points to the axis at b = 1, revealed the weakened interaction of O_2 and H_2O with the AC electrode. Although, the values of the solid points paradoxically again deviate from 1 right after crossing the intersection, where the AC electrode has been nearly free from the oxidative effect.

Furthermore, the open circuit potential (OCP) of the AC electrode of mass loading of 2.1 mg in electrochemical glass cell with and without N_2 flow is recorded in Fig. 3, after conditioning the electrode at 0 V for 10 min. From the onset of curve, a rapid drop in the electrode potential showed without external bias for N_2 flow into the electrolyte, which corresponds to the self-discharging of AC at 0V. After 6 hours, the OCP curve attained a plateau lasting for another 6 hours at -0.2V, indicating that the spontaneous adsorption of lithium ions onto the surfaces of AC largely ended. Whereas, the potential tracking in the presence of air revealed a tendency to equilibrium at positive potential. It is obvious that a potential of -0.2V is close to the potential at which the intersection lies in Fig. 2d. Being with a state of self-discharging makes it easier for AC to accommodate lithium ions during cathodic scans and more difficult to desorb lithium ions during anodic scans. Herein, the slight deviation of b values from 1 for solid points in Fig. 2d to the right of the intersection, would also be ascribed to the self-discharging of AC.

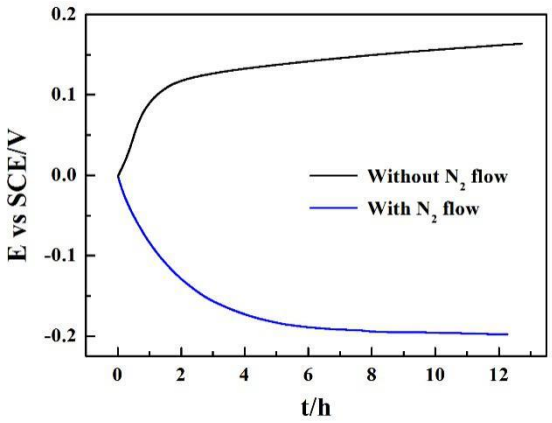

Figure 3. An OCP curve of the Activated carbon electrode of mass loading of 2.1mg tested in electrochemical glass cell with and without N_2 flow, after conditioning the electrode at 0V for 10min.

Fig 4 shows the typical galvanostatic charge-discharge curves for the AC electrode of mass loading of 2.1mg tested in electrochemical glass cell with and without N_2 flow within a potential window of 0 to -0.85V at a current density of 3.5C (1C = 55mAh/g). The discharge capacity of AC is 145mAh/g with a coulombic efficiency of 332% when it was discharged up to −0.85V in the presence of air. After

elimination of dissolved oxygen, an enormous 63% reduction in discharge capacity (53mAh/g) renders the coulombic efficiency relatively receptible, yielding a value of 106%. The result shows that whether the aqueous Li_2SO_4 electrolyte was exposed to air has a great influence on the performance of AC in it. In addition, the nonlinear discharge curve displayed in Fig 4b reflects the abnormal capacitive behavior of AC as well.

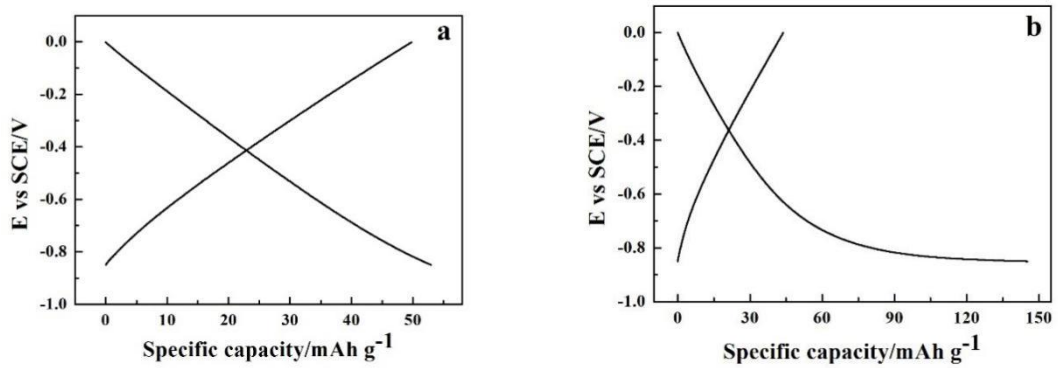

Figure 4. Galvanostatic charge-discharge curves of the Activated carbon electrode of mass loading of 2.1mg tested in glass cell (a) with and (b) without N_2 flow within a potential window of 0 to -0.85V at a current density of 3.5C (1C = 55mAh/g).

In recent years, a number of energy storage systems which were suitable for ALIHSs have been reported, and they all chose the carbon-based cathodes or anodes for the working principle of EDLCs [8, 17, 19, 20, 31-34]. The three-electrode cells were utilized to test the electrochemical behavior of those carbon materials in electrolyte via cyclic voltammetry (CV) before assembly of hybrid capacitor. Table 1 lists the relevant information from literature in terms of the operating conditions at which the electrochemical behavior of carbon materials were tested. The summary indicated that both charged and discharged carbon-based materials exhibited mostly electric double layer capacitive behavior at scan rates above 2mV/s in spite of various electrode mass loading [8, 19, 20, 31-34]. However, the circumstance similar with the present work was found. Ramkumar et al. [17] using the graphene like porous carbon (AC) synthesized from biomass as anode material for their studied system, the scan rate range of 0.1 to 1 mV/s was applied to obtain CV curves of AC. As a result, the considerable specific capacitance of AC which linearly decreased with increasing scan rates was attributed to the negligible relaxation time of the migration of lithium ion in bulk electrolyte, whereas the CV curve for scan rate of 0.1mV/s was nearly swallow by the negative current, no explanation was given to this unusual phenomenon and the capacitance reversibility concerned with other scans was not yet mentioned in the accepted manuscript. It is common knowledge that ALIHSs using electric double layer capacitance electrodes belong to the devices which are invented with the expectation of overcoming the power density limitation of LIBs, herein it was common to conduct CV at scan rates above 1mV/s or even approaching 100mV/s according to literature. As the LSV curves displayed in Fig 2b are symmetric rectangular shape, we assume that the plateaus of cathodic and anodic LSV curves are sufficiently flat such that the currents can be considered constant during scans. Obviously, the measure of preventing the electrolyte from air contact enhanced the rate performance of AC in a way reflected by the inconsistency

of pattern between the Fig 2a and b. Therefore, using the scan rates below 1mV/s to investigate the voltammetric property of discharged AC in aqueous Li_2SO_4 turns out to be necessary.

Table 1. Literature summary of experimental conditions applied in voltammetry to portray the electrochemical behaviors of the carbon-based cathodes/anodes utilized in energy storage systems suitable for Aqueous Lithium-ion Hybrid Supercapacitors device.

Energy storage system	**Electrolyte**	**Potential window**	**Scan rate ($mV\ s^{-1}$)**	**Mass loading ($mg\ cm^{-2}$)**	**Electrochemical behavior of carbon material**	**Ref. #**
Li_2NiTiO_4//AC	1M Li_2SO_4	-0.1 ~ 0.6 vs Ag/AgCl/V	10 for CV	N/A	Capacitive behavior with the CV curve of rectangular shape	[31]
$Li_{0.33}MnO_2$//AC	2M Li_2SO_4	0 ~ -1.1 vs SCE/V	5 for CV	N/A	Pure electric double layer capacitive behavior with the CV curves of rectangular shape	[32]
$LiMn_2O_4$/super P//AC	1M Li_2SO_4	0 ~ 0.6 vs SCE/V	2 for CV	6	Capacitive behavior with the CV curve of rectangular shape	[33]
$LiCoO_2$//AC $LiMn_2O_4$//AC $LiCo_{1/3}Ni_{1/3}Mn_{1/3}O_2$//AC	1M Li_2SO_4 with various pH values	0 ~ -0.85 vs SCE/V, pH 7 0~ -0.95 vs SCE/V, pH 9 0 ~ -1.05 vs SCE/V, pH 11 0 ~ -1.15 vs SCE/V, pH 13	10 for CV	N/A	Capacitive behavior with the CV curve of rectangular shape	[20]
$LiCo_{1/3}Ni_{1/3}Mn_{1/3}O_2$@C//AC	0.5M Li_2SO_4	0 ~ -1 vs Ag/AgCl/V	0.1 ~ 1 for CV	N/A	Mostly electric double layer capacitive behavior without further discussion for the Negative current swallowed CV curve for $0.1mV\ s^{-1}$	[17]
Li_xMnO_2//AC	1M Li_2SO_4	-0.3 ~ -1 vs SCE/V	2 ~ 100 for CV	5	Excellent reversibility with the CV curves of rectangular shape	[19]
$LiMn_2O_4$//graphene	1M Li_2SO_4	0 ~ -0.8 vs SCE/V	5 ~ 100 for CV	0.8	Ideal capacitive behavior with the CV curves of rectangular shape at all scan rates	[8]
$LiMnPO_4$/rGO//rGO	1M LiOH	0 ~ -1 vs Hg/HgO/V	5 for CV	3.6	Behavior of EDLCs with the CV curve of rectangular shape	[34]
N/A	0.5M Li_2SO_4	0 ~ -0.85 vs SCE/V	0.1 - 1 for LSV	0.8 - 5.7	The distortion of LSV curves was observed for the low mass loading (< $0.8mg\ cm^{-2}$) and scan rate (< $1mV\ s^{-1}$)	Present work

4. CONCLUSIONS

In this study, we have demonstrated experimentally that the electrolyte exposed to air has a considerable effect on the electrochemical performance of AC in aqueous 0.5M Li_2SO_4 solution at negative potentials. By applying a power-law equation, the oxidative effect of O_2 and H_2O was proposed to explain the abnormal capacitive behavior of AC in LSV test. In the electrolyte with N_2 flow, the electrochemical stability of AC was improved. The results show to enhance the rate performance as well as coulombic efficiency of AC, providing information of value based on application for ALIHSs using AC anode.

ACKNOWLEDGEMENTS
This work is supported by the National Natural Science Foundation of China (No. 11674085).

References

1. J. Lang, X. Zhang, B. Liu, R Wang, J. Chen and X. Yan, *J. Energy Chem*., 27 (2018) 43.
2. J. Zhang, Z. Shi and C. Wang, *Electrochim. Acta*, 125 (2014) 22.
3. J. Zhang, H. Wu, J. Wang, J. Shi and Z. Shi, *Electrochim. Acta*, 182 (2015) 156.
4. N.S. Choi, Z. Chen, S.A. Freunberger, X. Ji, Y.K. Sun, K. Amine, G. Yushin, L.F. Nazar, J. Cho and P.G. Bruce, *Angew. Chem., Int. Ed.*, 51 (2012) 9994.
5. H. Kim, M.Y. Cho, M.H. Kim, K.Y. Park, H. Gwon, Y. Lee, K.C. Roh and K. Kang, *Adv. Energy Mater.*, 3 (2013) 1500.
6. C. Qin, Y. Li, S. Lv, J. Xiang, C. Wang, X. Zhang, S. Qiu and G. Yushin, *Electrochim. Acta*, 253 (2017) 413.
7. R. Aswathy, T. Kesavan, K.T. Kumaran and P. Ragupathy, *J. Mater. Chem. A*, 3 (2015) 12386.
8. P. Pazhamalai, K. Krishnamoorthy, M.S.P. Sudhakaran and S.J. Kim, *ChemElectroChem*, 4 (2017) 396.
9. P. Pazhamalai, K. Krishnamoorthy, S. Sahoo and S.J. Kim, *J. Alloys Compd.*, 765 (2018) 1041.
10. K. Shree Kesavan, K. Surya and M.S. Michael, *Solid State Ionics*, 321 (2018) 15.
11. L.G.H. Staaf, P. Lundgren and P. Enoksson, *Nano Energy*, 9 (2014) 128.
12. B. Li, F. Dai, Q. Xiao, L. Yang, J. Shen, C. Zhang and M. Cai, *Adv. Energy Mater.*, 6 (2016) 1600802.
13. B. Li, F. Dai, Q. Xiao, L. Yang, J. Shen, C. Zhang and M. Cai, *Energy Environ. Sci.*, 9 (2016) 102.
14. W. Zuo, C. Wang, Y. Li and J. Liu, *Sci. Rep.*, 5 (2015) 7780.
15. F. Lou and D. Chen, *J. Energy Chem.*, 24 (2015) 559.
16. H. Wang, C. Guan, X. Wang and H.J. Fan, *Small*, 11 (2014) 1470.
17. B. Ramkumar, S. Yuvaraj, S. Surendran, K. Pandi, Hari Vignesh Ramasamy, Y.S. Lee and R. Kalai Selvan, *J. Phys. Chem. Solids*, 112 (2018) 270.
18. P. Chaturvedi, A. Sil and Y. Sharma, *Ionics*, 22 (2016) 1719.
19. L. Chen, L. Chen, W. Zhai, D. Li, Y. Lin, S. Guo, J. Feng, L. Zhang, L. Song, P. Si and L. Ci, *J. Power Sources*, 413 (2019) 302.
20. Y. Wang, J. Luo, C. Wang and Y. Xia, *J. Electrochem. Soc.*, 153 (2006) A1425.
21. Y. Wang and Y. Xia, *J. Electrochem. Soc.*, 153 (2006) A450.
22. H. Wang, M. Yoshio, A.K. Thapa and H. Nakamura, *J. Power Sources*, 169 (2007) 375.
23. Q.T. Qu, B. Wang, L.C. Yang, Y. Shi, S. Tian and Y.P. Wu, *Electrochem. Commun.*, 10 (2008) 1652.
24. F. Béguin, V. Presser, A. Balducci and E. Frackowiak, *Adv. Mater.*, 26 (2014) 2219.
25. W. Tang, L.L. Liu, S. Tian, L. Li, Y.B. Yue, Y.P. Wu, S.Y. Guan and K. Zhu, *Electrochem. Commun.*, 12 (2010) 1524.
26. W. Tang, S. Tian, L.L. Liu, L. Li, H.P. Zhang, Y.B. Yue, Y. Bai, Y.P. Wu and K. Zhu, *Electrochem. Commun.*, 13 (2011) 205.
27. Q. Qu, L. Fu, X. Zhan, D. Samuelis, J. Maier, L. Li, S. Tian, Z. Li and Y. Wu, *Energy Environ. Sci.*, 4 (2011) 3985.
28. J.Y. Luo, W.J. Cui, P. He and Y.Y. Xia, *Nat. Chem.*, 2 (2010) 760.
29. H. Lindström, S. Södergren, A. Solbrand, H. Rensmo, J. Hjelm, A. Hagfeldt and S.E. Lindquist, *J. Phys. Chem. B*, 101 (1997) 7717.
30. V. Augustyn, J. Come, M.A. Lowe, J.W. Kim, P.L. Taberna, S.H. Tolbert, H.D. Abruña, P. Simon and B. Dunn, *Nat. Mater.*, 12 (2013) 518.
31. S.R. Anslin, M.S. Michael and S.R.S. Prabaharan, *Materials Today: Proceedings*, 5 (2018) 23339.
32. R. Attias, O. Hana, D. Sharon, D. Malka, D. Hirshberg, S. Luski and D. Aurbach, *Electrochim. Acta*, 254 (2017) 155.

33. L. Chen, W. Zhai, L. Chen, D. Li, X. Ma, Q. Ai, X. Xu, G. Hou, L. Zhang, J. Feng, P. Si and L. Ci, *J. Power Sources*, 392 (2018) 116.
34. L. Xu, S. Wang, X. Zhang, T. He, F. Lu, H. Li and J. Ye, *Appl. Surf. Sci.*, 428 (2018) 997.